

Current transport studies of ZnO/*p*-Si heterostructures grown by plasma immersion ion implantation and deposition

X. D. Chen, C. C. Ling,^{a)} S. Fung, and C. D. Beling

Department of Physics, The University of Hong Kong, Pokfulam Road, Hong Kong, Peoples's Republic of China

Y. F. Mei, Ricky K. Y. Fu, G. G. Siu, and Paul. K. Chu

Department of Physics and Materials Science, City University of Hong Kong, Kowloon, Hong Kong, Peoples's Republic of China

(Received 29 November 2005; accepted 1 March 2006; published online 27 March 2006)

Rectifying undoped and nitrogen-doped ZnO/*p*-Si heterojunctions were fabricated by plasma immersion ion implantation and deposition. The undoped and nitrogen-doped ZnO films were *n* type ($n \sim 10^{19} \text{ cm}^{-3}$) and highly resistive (resistivity $\sim 10^5 \Omega \text{ cm}$), respectively. While forward biasing the undoped-ZnO/*p*-Si, the current follows Ohmic behavior if the applied bias V_{forward} is larger than $\sim 0.4 \text{ V}$. However, for the nitrogen-doped-ZnO/*p*-Si sample, the current is Ohmic for $V_{\text{forward}} < 1.0 \text{ V}$ and then transits to $J \sim V^2$ for $V_{\text{forward}} > 2.5 \text{ V}$. The transport properties of the undoped-ZnO/*p*-Si and the N-doped-ZnO/*p*-Si diodes were explained in terms of the Anderson model and the space charge limited current model, respectively. © 2006 American Institute of Physics.

[DOI: 10.1063/1.2190444]

Zinc oxide (ZnO) is a wide-band-gap semiconductor having properties suitable for various applications such as ultraviolet (UV) optoelectronic devices, transparent high power and high frequency electronic devices, surface acoustic wave devices, piezoelectronic transducers, and chemical gas sensors. ZnO film has been fabricated with various methods such as molecular beam epitaxy (MBE), chemical vapor deposition (CVD), radio frequency (rf) magnetron sputtering, pulsed laser deposition or electron evaporation, and on different substrates such as silicon, sapphire, or silicon carbide. Detailed reviews on ZnO material and device were given in review articles such as Refs. 1–4. Undoped ZnO material is of *n* type and doping the material *p* type is rather difficult. Nitrogen has been considered to be the *p*-type dopant of the material. Look *et al.* firstly demonstrated that MBE grown ZnO on a Li-doped semi-insulating (SI) ZnO substrate doped with the O and N fluxes created by a rf plasma yielded a hole concentration of $9 \times 10^{16} \text{ cm}^{-3}$ and a hole mobility of $2 \text{ cm}^2 \text{ V}^{-1} \text{ s}^{-1}$.⁵ However, in some cases, the resulting materials were highly resistive and no definite *p*-type nature was observed.^{6,7}

Although understanding the electrical properties of the ZnO related system is important for successful material and device fabrications, electrical transport of ZnO material or ZnO based structure has not yet been extensively studied nor thoroughly understood. In the present study, we have fabricated highly oriented undoped and nitrogen-doped (100) ZnO film on *p*-type silicon by plasma immersion ion implantation with deposition (PIII&D),⁸ and the resulting ZnO films were respectively *n* type and highly resistive. The electrical characters of the sample films were studied and the physics of carrier transport was investigated in detail.

ZnO (0001) films were fabricated on *p*-type silicon by PIII&D. The substrate used in the present experiment was *p*-type (100) Si wafer with a resistivity of 10–30 $\Omega \text{ cm}$. The plasma immersion ion implanter used in the present study

was equipped with a cathodic arc source. The base pressure was kept at 1×10^{-5} Torr during the operation. In order to reduce the detrimental macroparticles, the zinc plasma formed at the cathodic arc source was guided through a magnetic filter and was drifted into the vacuum chamber. A dual plasma consisting of zinc and oxygen ions was formed as oxygen gas was simultaneously blend into the vacuum. In order to dope the material, mixing gas of oxygen and nitrogen (ratio $\text{O}_2:\text{N}_2$:10:10, flow rate: 20 SCCM (SCCM denotes cubic centimeter per minute at STP), pressure: $\sim 1.0 \times 10^{-3}$ Torr) was introduced into the vacuum chamber. X-ray diffraction measurements showed that all the ZnO films were highly oriented in the (0002) direction, and no other ZnO related diffraction peaks were observed. The full width at half maximum (FWHM) of the (0002) ZnO peak observed in the x-ray diffraction spectra was as narrow as 0.21° , implying that the grown films had a very high degree of crystallinity.

Room temperature Hall measurements were performed on the undoped and the N-doped samples with the Van de Pauw configuration. Ohmic contacts on the ZnO and the *p*-type Si surfaces were fabricated by the thermal evaporation of Al and In metals, respectively. The Hall measurement showed that the undoped ZnO film was *n*-type having electron concentration and mobility of $2.3 \times 10^{19} \text{ cm}^{-3}$ and $120 \text{ cm}^2 \text{ V}^{-1} \text{ s}^{-1}$, respectively. The nitrogen-doped ZnO film was found to be highly resistive having a resistivity of $\sim 10^5 \Omega \text{ cm}$, thus introducing the difficulty of accurately determining the carrier type by the Hall method.

Current-voltage (*I*-*V*) characteristic across the ZnO/*p*-Si junctions were studied (i.e., the *AB* measurement as shown in Fig. 1). The convention of the applied bias polarity was defined as negative at the ZnO side and earthed at the *p*-Si side. The *I*-*V* data of the undoped and the nitrogen-doped ZnO/*p*-Si junction were shown in Fig. 1, for which rectifying character was observed on both of the junctions. The threshold voltage for the undoped-ZnO/*p*-Si diodes is $\sim 0.4 \text{ V}$. The room temperature leakage currents with 8 V

^{a)}Electronic mail: ccling@hku.hk

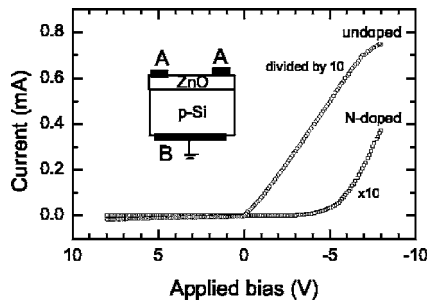


FIG. 1. *I-V* data of the undoped-ZnO/*p*-Si and the N-doped-ZnO/*p*-Si heterostructures measured at room temperature.

reverse bias applied for the undoped and the nitrogen-doped samples were found to be 10 μ A and 3 nA, respectively.

The forward current transport property of the undoped-ZnO/*p*-Si sample was investigated at different temperatures varying from 200–370 K. The current as a function of the applied bias and also the corresponding diode resistance defined as $R=dV/dI$ for the forward bias region are shown in Fig. 2. Below the threshold voltage, R decreases with increasing forward bias. It maintains a constant resistance value above the threshold voltage. It is also noted that threshold voltage decreases with increasing temperature. Assuming the continuity of vacuum levels, neglecting the effects of dipole and interfacial state, the heterojunction band structure of the undoped-ZnO/*p*-Si can be constructed by the Anderson model.⁹ Values of electron affinity of $\chi(\text{ZnO})=4.4$ eV (Ref. 10) and $\chi(\text{Si})=4.6$ eV band gaps of $E_g(\text{ZnO})=3.4$ eV and $E_g(\text{Si})=1.1$ eV were taken. The band structure of such a heterojunction is shown in Fig. 3. As shown in Fig. 3, the barrier for electron is equal to $\Delta E_C=\chi(\text{ZnO})-\chi(\text{Si})=-0.3$ eV and that for hole is equal to 2.8 eV. Both the conduction band and the valance band have band offsets which are originated from the difference in the electron affinities and the band gaps of the two materials. It is noticed that the valance band offset ΔE_V is much larger than the conduction band offset ΔE_C . As the carrier concentration of the *p*-Si is much lower than that of the undoped ZnO, the depletion space charge region mainly locates at the *p*-Si side. As the ZnO side is under the negative bias, the conduction band barrier will be decreased and will enhance the electron flow from the ZnO to the *p*-Si. The subsequent recombination at the *p*-Si depletion region would give rise to the forward bias current flow. This implies that the diode resistance would firstly decrease upon the increase of the forward bias voltage (i.e., the lowering of the barrier). As the forward bias

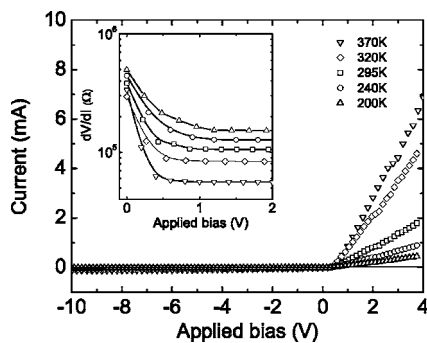


FIG. 2. *I-V* data of the undoped-ZnO/*p*-Si sample measured at different temperatures. The inset showed the diode resistance dV/dI as a function of the applied bias as the sample was forward biased.

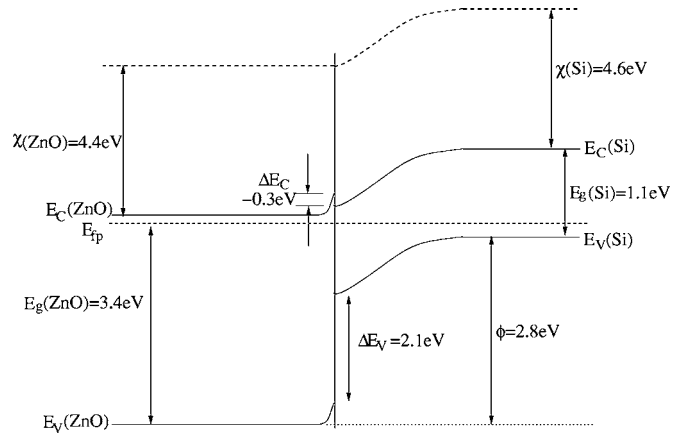


FIG. 3. Band structure of the ZnO/*p*-Si heterostructure derived from the Anderson model.

is large enough, the barrier would essentially be negligible, the *I-V* behavior thus becomes Ohmic, and the diode resistance becomes constant, which is contributed from the series bulk material resistance.

The log-log plot of the *I-V* data for the nitrogen-doped-ZnO/*p*-Si sample is shown in Fig. 4. The current transport follows an Ohmic behavior (i.e., $J \sim V$) for the applied forward voltage smaller than ~ 1 V. As the applied bias is larger than ~ 1.0 V, the current transport deviates from Ohmic behavior and with applied bias larger than ~ 2.5 V, it follows the dependence of $J \sim V^2$. The $J \sim V^2$ transport of the N-doped-ZnO/*p*-Si cannot be explained by the heterojunction band structure model as described in the last paragraph.

Space charge limited (SCL) current conduction has been observed in various semiconductor structures.^{11–14} Lambort and Mark¹⁵ have developed the single carrier SCL current model with the presence of a trap above the Fermi level. As the applied voltage is lower than the onset voltage for deviating from Ohmic behavior (i.e., $V < V_{on}$ as shown in Fig. 4), the thermally generated carrier density n_0 dominates over the injected carrier density and the carrier transit time $\tau_c = d^2/\mu V_{on}$ is larger than the dielectric relaxation time $\tau_d = \epsilon/qn\mu$. The injected carrier would thus undergo dielectric relaxation to maintain the charge neutrality rather than transport across the sample. In this region, the traps are not completely filled. As the applied voltage is larger than V_{on} , τ_c is smaller than τ_d and the injected carrier dominates over the thermally generated carrier. The increase of the applied voltage also shifts the quasi-Fermi level towards the conduction

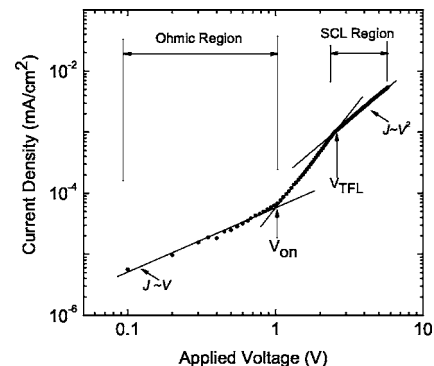


FIG. 4. The log-log plot for the *I-V* data of the N-doped-ZnO/*p*-Si sample at room temperature.

band and the effect would be the filling up of the trap at the energy level of $E_C - E_t$ (i.e., the trap filling region $V_{on} < V < V_{TFL}$ in Fig. 4). As the applied voltage further increases to the extent that all the traps are filled (i.e., $V > V_{TFL}$ in Fig. 4), the conduction would become space charge limited and the current follows the dependence¹⁵ of $J = (9/8)\epsilon\mu V^2/d^3$, where d is the thickness of the active region.

As for the present N-doped-ZnO/*p*-Si structure under the forward bias, most of the applied bias potential would drop across the ZnO film as its resistance is high. Because of the large barrier to hole injection as compared to that of electron, the injection current is mainly carried through the injected electrons, which is of the form of the single carrier injection. The activation energy of the trap $E_C - E_t$ can be found by plotting $\log J$ against $1/T$ in the trap filling region and the activation energy of the trap was found to be 0.43 eV. By monitoring the trap fill limit voltage which is given by,¹⁵ $V_{TFL} = qN_t d^2 / 2\epsilon$, the trap concentration N_t was found to have a value of $(2-3) \times 10^{17} \text{ cm}^{-3}$.

In conclusion, we have fabricated the undoped and the nitrogen-doped-ZnO/*p*-Si heterojunction by PIII&D. The undoped and the nitrogen-doped ZnO films were *n* type and highly resistive. Both of the samples showed rectifying behavior. The forward *I-V* data showed that the undoped-ZnO/*p*-Si sample followed the Ohmic behavior. However, for the N-doped-ZnO/*p*-Si sample, the current is proportional to V^2 , which is a typical behavior of the space charge limited current phenomenon.

This project was supported by the CERG, RGC, HKSAR (No. 7032/04), the University Development, Hong Kong University, and the City University of Hong Kong Direct Allocation Grant No. 9360110.

¹D. C. Look, *Mater. Sci. Eng., B* **80**, 383 (2001).

²Chris G. Van de Walle, *Physica B* **308-310**, 899 (2001).

³S. J. Pearton, D. P. Norton, K. Ip, Y. W. Heo, and T. Steiner, *Prog. Mater. Sci.* **50**, 293 (2005).

⁴U. Ozgur, Ya. I. Alivov, C. Liu, A. Teke, M. A. Reshchikov, S. Doğan, V. Avrutin, S. J. Cho, and H. Morkoç, *J. Appl. Phys.* **98**, 041301 (2005).

⁵D. C. Look, D. C. Reynolds, C. W. Litton, R. L. Jones, D. B. Eason, and G. Cantwell, *Appl. Phys. Lett.* **81**, 1830 (2002).

⁶K. Minegishi, Y. Koiwai, Y. Kikuchi, K. Yano, M. Kasuga, and A. Shimizu, *Jpn. J. Appl. Phys., Part 2* **36**, L1453 (1997).

⁷K. Iwata, P. Fons, A. Yamada, K. Matsubara, and S. Nike, *J. Cryst. Growth* **209**, 526 (2000).

⁸Y. F. Mei, R. K. Y. Fu, G. G. Siu, P. K. Chu, Z. M. Li, C. L. Yang, W. K. Ge, Z. K. Tang, W. Y. Cheung, and S. P. Wong, *Mater. Sci. Semicond. Process.* **7**, 459 (2004).

⁹A. G. Milnes and D. L. Feucht, *Heterojunctions and Metal-Semiconductor Junctions* (Academic, New York, 1972).

¹⁰A. Aranovich, D. G. Golmayo, A. L. Fabrenbruch, and R. H. Bube, *J. Appl. Phys.* **51**, 4260 (1980).

¹¹O. J. Marsh and C. R. Viswanathan, *J. Appl. Phys.* **38**, 3135 (1967).

¹²S. Tehrani, J. S. Kim, L. L. Hench, C. M. Van Vilet, and G. Bosman, *J. Appl. Phys.* **58**, 1562 (1985).

¹³H. P. Hall, M. A. Awaah, and K. Das, *Phys. Status Solidi A* **201**, 522 (2004).

¹⁴R. L. Hoffman, J. F. Wagner, M. K. Jayaraj, and J. Tate, *J. Appl. Phys.* **90**, 5763 (2001).

¹⁵M. A. Lampert and P. Mark, *Current Injection in Solids* (Academic, New York, 1970).